

Quantitative characterization of the microstructure of advanced materials

K.J. KURZYDŁOWSKI

*Warsaw University of Technology
Department of Materials Science and Engineering
Wolowska 141, 02-507 Warsaw, Poland*

Advanced materials contain particles, grains and pores, interfaces, grain boundaries and other microstructural elements. Depending on the details of the technological route they differ in the amount and the distribution of these elements. Such differences can be now analysed in a quantitative way using the methods of image analysis and stereology. In particular, these methods provide estimates of the number of microstructural elements of a given size (e.g. number of particles per unit volume), their shape (if applicable), and their spatial distribution. The paper describes methodology of these measurements, and how the results can be applied to optimise microstructure of advanced materials.

Key words: principles of microstructure quantification, stochastic approach, stereology, image analysis.

1. Introduction

1.1. Microstructure of materials

Materials science is a field of scientific pursuit that concentrates attention on the relationships between microstructure and properties of materials. The term microstructure in this context is used to describe a set of characteristic elements that can be identified in the arrangement of atoms and/or molecules forming a given material. Depending on the type of the material studied these elements may consist of single atoms, groups of atoms and large aggregates of atoms or molecules. Examples of microstructural elements of modern materials include in particular:

- dislocations in crystals and fibers in composites,
- interfaces such as grain- and inter-phase-boundaries,
- particles in composites and grains in polycrystals.

Images of the above listed microstructural elements are shown in Fig. 1.

1.2. Classification of the microstructural elements

There are a number of different classifications of microstructural elements used in different texts. However, the most general and most suitable for the present text seems to be the one based on the analysis of their dimensions. Microstructural elements can be broadly divided into four categories:

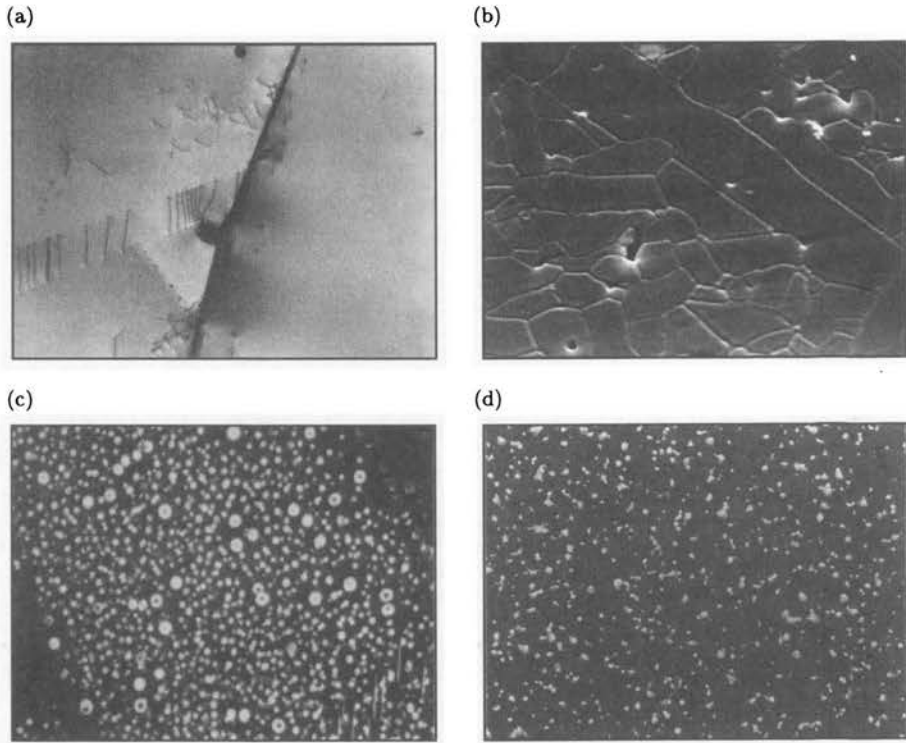


FIGURE 1. Electron microscope images of the microstructure of engineering materials:
 (a) dislocations in corrosion resistant iron-chromium alloy (TEM),
 (b) grain boundaries in Al₂O₃ ceramic (SEM),
 (c) strengthening particles in Al-Li alloy,
 (d) particles of metal in ceramic-matrix-composite.

TABLE 1. Elements of microstructure for selected types of materials.

Type of material	0-dimensional elements	1-dimensional elements	2-dimensional elements	3-dimensional elements
polycrystals	vacancies, impurities, alloying atoms	dislocations	stacking faults, grain boundaries, free surfaces, interfaces, cracks	domains, grains, aggregates, second-phase particles, pores
composites	small voids, particles	fibers	interfaces, lamellar particles	particulates, voids

- point – 0 dimensional,
- linear – 1 dimensional,
- surface – 2 dimensional,
- volume – 3 dimensional.

Examples typical of each category are given in Table 1, which lists the most commonly distinguished elements of the microstructure of modern materials.

Characterization of the microstructure of materials involves identification of the main microstructural elements present and a quantitative description of their sizes, shapes, numbers and positions within the specimen of the studied material. In other words this is a process that answers the following questions:

1. What are the elements in the internal structure of a given material that distinguish it from other materials of that kind (of say similar chemical composition)?
2. Where are these elements located and in what quantity?
3. What is their size and shape?

Answers to all these questions provide a comprehensive description of the material microstructure that can be used to explain its properties and to gain better control over its technological usage. However, the first of these questions is a domain of material physics. In fact, microstructural elements such as dislocations and grain boundaries by themselves have become subjects of extensive theoretical studies. In the present text the focus is placed on the two last questions.

1.3. Microstructure vs. properties

One of the foundations of modern materials science is the recognition of the fact that the properties of materials are related to their microstructure. This general statement can be illustrated, for example, by the correlations between microstructure and properties of two-phase materials which are widely used in technological applications. This is due to the fact that it is increasingly possible to “design” microstructures which deliver the combination of properties desired. Perhaps the best examples of this come from the field of composite materials where some of the simpler properties (such as stiffness/elastic modulus, density) are determined by linear combinations of the parameters describing properties of the respective phases and their volumetric content:

$$X_{AB} = (V_V)_A X_A + (V_V)_B X_B. \quad (1.1)$$

In this equation X_{AB} stands for a given property of the two-phase material, (V_V) for volume fraction of a given component and X_A , X_B define properties of the components (e.g. elastic modulus, density, hardness).

Another example of the microstructure-property relationships concerns resistance to plastic deformation of polycrystals. Polycrystals are aggregates of large numbers of crystals (grains). They constitute a significant fraction of the materials used for a variety of applications. This group includes metals, ceramics, intermetallics as well as some types of polymer. The grains and the grain boundaries are one of the elements of the microstructure of polycrystals. The dimensions of the grains (and the grain boundaries) may vary from millimeters down to nanometers.

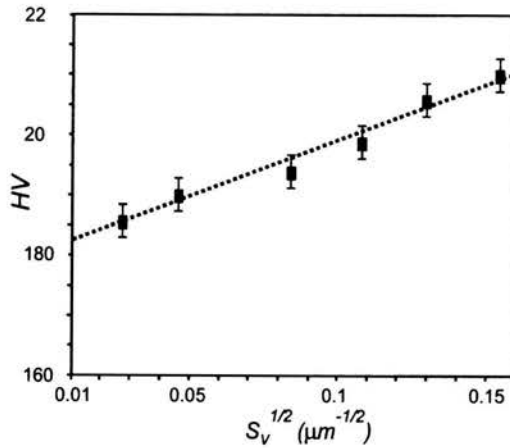


FIGURE 2. Correlation between the surface area of the grain boundaries in unit volume and the hardness of an iron-chromium alloy.

One of the simple measures of the resistance of polycrystals to plastic deformation is the hardness test. Some hardness tests, such as Vickers and Brinell, yield a number that defines the resistance to plastic deformation in MPa. Figure 2 presents the results of Vickers tests carried out on a series of specimens of a single-phase FCC alloy with different grain sizes. The hardness is plotted against the square root of the grain boundary area in unit volume, $(S_V)^{1/2}$. The data support the following formula:

$$H = H_o + K_H(S_V)^{1/2}. \quad (1.2)$$

This formula, known as the Hall-Petch relationship, is one of the most useful in the field of physical metallurgy. It can be used to predict the properties of a wide range of materials including metals, ceramic, intermetallics and polymers.

1.4. Stochastic character of the geometry of microstructural elements

One of the important properties of the microstructures of materials – the stochastic character of their geometry (the term stochastic is used here to underline the fact that the geometry of the microstructural elements shows a degree of randomness, stochastic = random). Particles and grains differ in their size and shape and form populations characterized by distributions of parameters defining them. An example of diversity in size and shape of microstructural elements is given in Fig. 3 which shows images of the Al_2O_3 sinters produced employing different technologies.

The stochastic character of the geometry of microstructural elements means that their description requires the application of statistical methods, which brings in with it the concepts of distribution functions, estimators and intervals of confidence. Looking at some consequences of such a situation, it should be noted that as a result of their stochastic character the elements cannot be characterized by single numbers of an unconditional character. In order to describe the microstructure we are forced

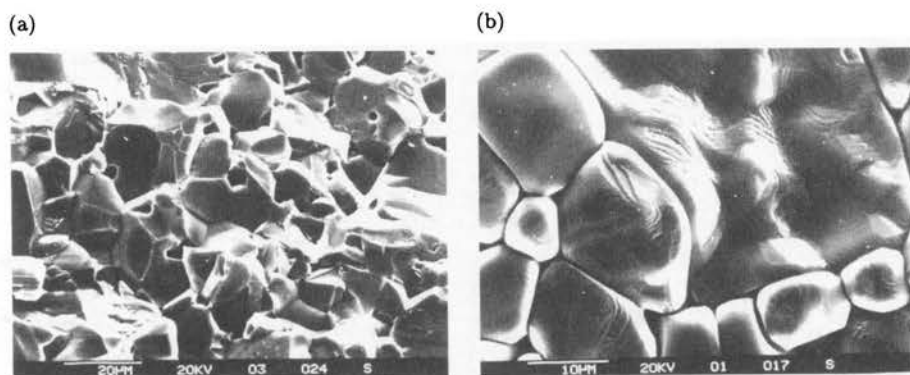


FIGURE 3. Scanning electron microscope image of the Al_2O_3 sinters produced via standard method (a) and (b) using activators of sintering (boron compounds).

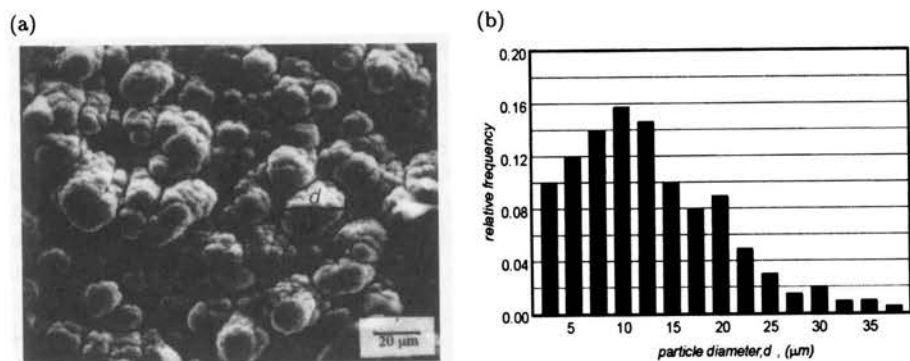


FIGURE 4. SEM image of thin film, TiN, on the surface of metallic substrate. Each spherical element can be characterized by diameter d , as explained in (a). The experimental frequency of d , $f(d)$, is given in (b).

to use figures derived from a set of data, for example the mean, median, standard deviation etc., see Fig. 4.

It should be also noted that, in most cases the populations of the microstructural elements are too big to be studied at the 100% level. Instead we conduct our studies on samples, i.e. finite subsets of populations. This means that we usually have to deal with restricted information about the objects studied and are forced to design thoughtfully the procedures for sampling elements to be selected for the measurements from the whole population.

1.5. Relation between 3D structure and 2D image – stereology

The elements of a microstructure extend into 3-dimensions and are distributed over the volume of the specimen. This means that characterization of the microstructural elements should be based on some 3-dimensional model for the material studied. On the other hand, in an experimental approach they are commonly studied

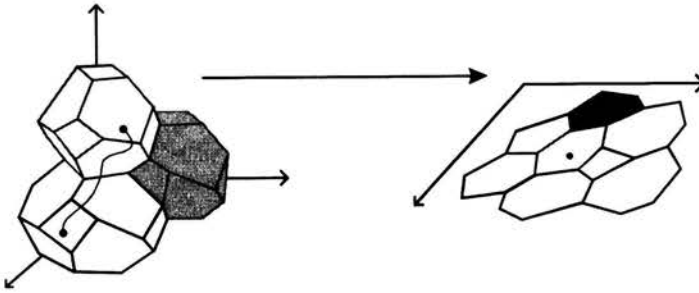


FIGURE 5. Dimensionality reduction during imaging of the microstructural elements: reduction of the 3D particles into 2D elements, transformation of 2D interfaces into lines, reduction of 1D lines into points.

on 2-dimensional cross-sections or via examination of thin slices. This leads to reduction in the dimensionality of the microstructural elements as shown in Fig. 5.

In modern materials science observations are made frequently on a cross-section by reflecting the light illuminating the specimen; scanning electron microscopy involves analysis of the signals coming from the surface activated by an electron beam; while transmission electron microscopy provides information on the microstructure of slices with a thickness of a fraction of a micrometer. On the other hand a large number of properties are related to microstructural elements which are distributed over the volume of the material. In this situation, the required 3-dimensional description of the microstructure is inferred from the 2-dimensional images by means of the methods of quantitative stereology.

According to a dictionary stereology is "... a branch of science concerned with the development and testing of inferences about the three dimensional properties... from a two-dimensional point-of-view...". In this context the term quantitative is used to indicate that the inferences mentioned in the definition are to be of a quantitative nature.

The term stereology has been introduced in the early sixties, however, the foundations of the discipline existed before. In fact the first accounts of a systematic stereological approach go back to the end of the first part of XIX-th century when Delesse solved the problem of volume fraction measurements through measurements of aerial density of the profiles of features. In the 1920s, Wicksell developed a formula for estimating the number of particles in the volume of a material from measurements of their section densities and in the 1940s, Saltykov derived a relationship that could be used to determine the specific surface area of particles in a given volume. These theoretical results in the field were not disseminated across the various branches of the science and characteristically the methods were discovered and re-discovered independently. The year 1961 is noted by the foundation of International Society for Stereology. In subsequent years the Society has organized a large number of conferences, congresses and seminars that have helped to accelerate progress in the theoretical foundations of stereology and to spread their knowledge among scientists working in different fields of biology, medicine, geography, geology and materials science.

A quantitative description of the properties of two-dimensional images of microstructures are a prerequisite for the quantitative inference of the properties of the 3-dimensional microstructure. In the past, a number of methods have been developed that allow an appropriate quantitative characterization of two-dimensional images by means of simple counting methods. In recent years significant progress has been made in developing automatic computer-aided procedures.

2. Principles of stereology – polycrystals

2.1. Characterization of the grains and particles

Basic stereological methods are based on the measurements carried out on images of the microstructures. Their extensive description can be found, for example, in [1 and 2]. The following text is focused on characterization of the grains and particles in the engineering materials.

Grains forming a 3D polycrystal are volumetric elements. They can be described primarily in terms of their volume, V_i , and surface, S_i . As a result of the space filling requirement, the surfaces of the grains are divided into faces, S_{ij} , and each face is shared by two neighboring grains with indices i and j . The term "grain boundary" in most cases is used to refer to any of the faces of a grain. Faces of grains meet along common edges, (grain edges), E_{jkl} , at which at least three grains (j, k, l) are joined. The edges E_{jkl} are connected at points, C_{pqrs} , termed vertices (grain corners). If observed on sections, 3D polycrystals give images which have characteristics of a 2D polycrystalline appearance.

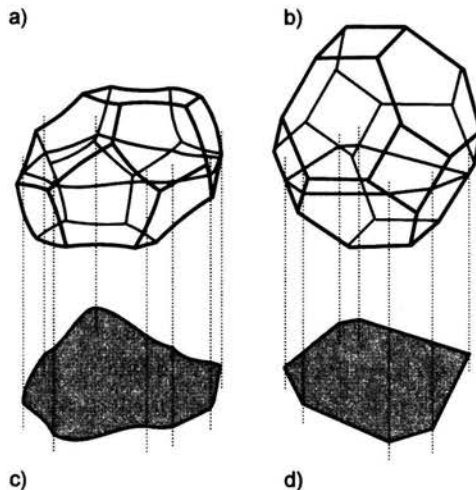


FIGURE 6. The relationship between the 3D geometry of the grains in polycrystals and images of their sections:

- (a) typical shape of grains,
- (b) relatively simple 3D polyhedra used for their modelling,
- (c) images of sections of grains,
- (d) images of polyhedra used for modelling grain geometry.

2D polycrystals contain planar grains which are characterized by grain area, A_i (or equivalent circle diameter, d_2 , such that $4A = \pi d_2^2$), and grain perimeter, p_i . Grain perimeter is divided into grain boundary segments, l_{ij} , which are joined at triple points, T_{ijk} . A 1D polycrystal is described by the length of its grains, L . All these parameters are further explained in Fig. 6.

Due to the 3D character of grains, direct studies of their geometry in non-transparent materials would require separation of polycrystal into individual grains. This has been achieved for some metal systems by reducing the strength of grain boundaries. An alternative to grain separation is the method of serial sectioning coupled with procedures which make it possible to re-construct 3D geometry from 2D sections – see Fig. 7.

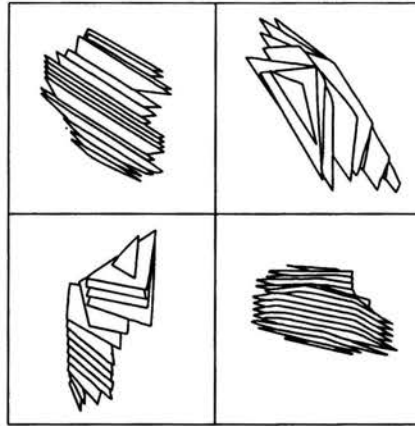


FIGURE 7. An example of 3D reconstruction of the geometry of grains in polycrystalline materials.

In materials science size of grains in polycrystalline aggregates can be describe using one, or a combination, of the following parameters:

- grain volume, V ;
- grain section area, A ;
- grain boundary area in unit volume, S_V ;
- intercept length, l .

The choice of the parameter is usually determined by the needs of a theoretical model of the material and its properties. For example:

- grain volume is measured if the focus is on the properties which depend on the volume of the individual grains, e.g. electron and X-ray diffraction;
- intercepts are measured, if the size of grains is analyzed in the context of dislocation pile-ups;
- grain surface is quantified, if one is interested in the total amount of grain boundaries per unit volume of the material.

Nowadays the measurements of the grain size are carried out with the aid of computerized image analyzers. Various parameters describing the grain size are

interdependent and one can be linked to the others using principles of stereology (see for example [1,2]). Stereological methods and image analysis can be also employed to quantify the shape of grains.

2.2. Grain boundary area

For most applications in materials science the grain size is sufficiently well defined by the value of the mean grain size. Depending on the parameter in question it can be mean volume, $E(V)$, mean section area, $E(A)$ or mean intercept, $E(l)$. It should be noted that the grain boundary area in unit volume, S_V , is a mean parameter by definition. This is due to the fact that unlike the three others it is not measured for individual entities (grains, grain sections and intercepts).

The mean intercept length is measured by counting the intersection points of test lines with the grain boundary network revealed on sections of polycrystals. Parallel lines on a random section can be used where the grain geometry is isotropic. It should be stressed, however, that in the case of anisotropic grain structures it is necessary to use a system of lines randomly oriented in 3-D. This criterion is fulfilled by the method based on vertical section in which test lines are used in the form of cycloids. An example of the mean intercept measurements for isotropic and anisotropic grain structures are shown in Fig. 8.

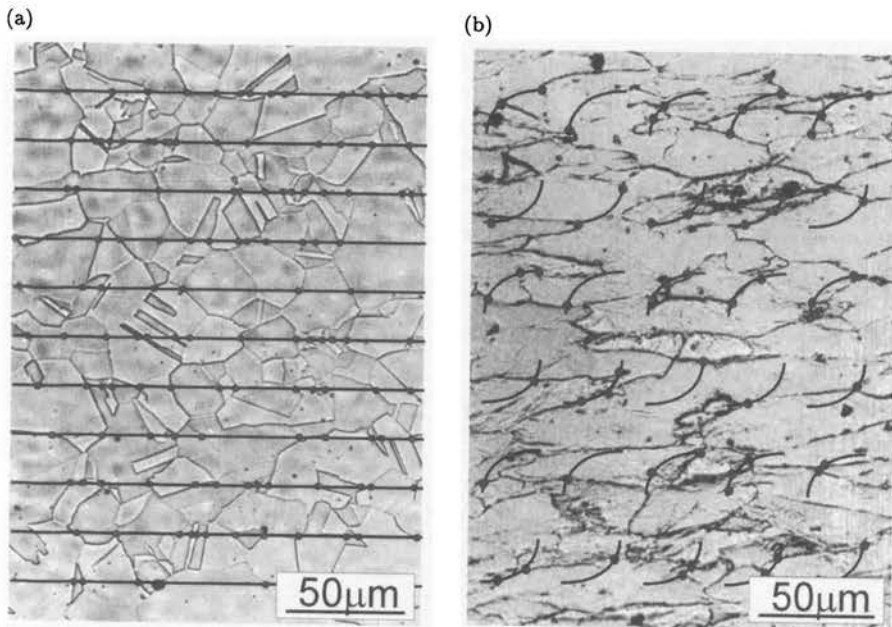


FIGURE 8. Explanation of the measurements of grain boundary area in unit volume:
(a) isotropic, (b) anisotropic polycrystals.

The mean intercept length, $E(l)$, if used for 3-dimensional polycrystals poorly describes the size of individual grains. It can be used as a scale parameter to quantify

grain size only in self-similar grain structures which can be obtained from a "basic pattern" by changing its magnification. However, its importance, apart from simplicity, is related to the stereological equation that relates $E(l)$ to surface-to-volume ratio, S_V :

$$E(l) = \frac{2}{S_V}. \quad (2.1)$$

It should be also pointed out that S_V can be used to obtain estimation of the volume occupied by so called grain-boundary-phase. (The volume of the grain-boundary-phase in unit volume is given as $S_V h$, where h is the "thickness of the grain boundaries").

The grain section area, A , is perhaps one of the most frequently parameters for grain structures. The value of grain section area, and in turn equivalent area diameter, d_2 , can be directly measured from micrographs of the grain boundary network by planimetric methods or by the procedure of counting the number of grains in a unit area, N_A . It should be pointed, however, that neither the mean value of A , the mean value of d_2 , nor the density of the grains, N_A are proper measures of the grain size¹⁾. The major reason for that is that large grains are over-represented on sections of polycrystals. This problem can be solved if the measurements of the grain section area are analyzed along the rules of stereology (see for example [3]) and are used to determine the true 3D average diameter.

2.3. Disector

The true volume of grains, $E(V)$, can be estimated with the help of the DISECTOR method. This procedure requires, in general, serial sectioning of the material as its principle is to count the grains below a cross-section instead of the grains cut by the cross-section – see Fig. 9.

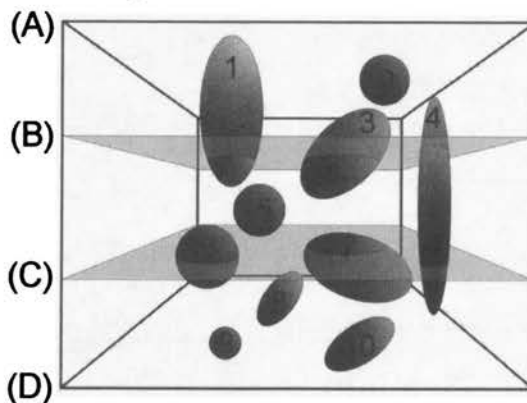


FIGURE 9. Explanation of the DISECTOR method. Between the planes (B) and (C) we can observe 6 particles. But only 3 (5, 6, 7) are cut by plane (B). These three we can include to the volume between (B) and (C). The other contains the volume between (A) and (B) – 4 particles (1, 2, 3, 4). Similarly, between (C) and (D) we can count the particles (8, 9, 10).

¹⁾ In fact the latter parameter, N_A , describes the mean curvature of grains.

The volume-weighted mean volume of grains, $E_V(V)$, in which large grains are slightly over-represented, can be determined by the procedure proposed by Jensen and Gundersen [4]. This procedure requires random point sampling of the grains revealed on a cross-section and subsequent measurements of the length intercepts, l_i , drawn through the points, P_i "thrown" on the image of the grain boundaries, as shown schematically in Fig. 10. On the basis of such measurements the mean volume, $E_V(V)$, can be estimated using the formula:

$$E_V(V) = \frac{\pi}{3} E(l^3). \tag{2.2}$$

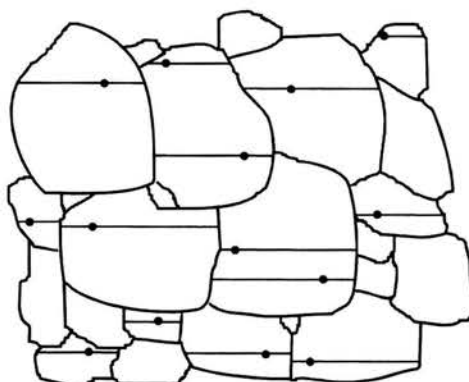


FIGURE 10. Explanation of the point-sampled-intercept method.

3. Grain size uniformity

Grains in polycrystals differ in their volume and the same mean size can be ascribed to geometrically different populations of grains. A simple measure of grain size uniformity is the variance of the grain size distribution function $\text{VAR}(V)$, or standard deviation $\text{SD}(V)$, and coefficient of variation $\text{CV}(V)$:

$$\text{CV}^2(V) = \frac{\text{VAR}(V)}{[E(V)]^2}. \tag{3.1}$$

Another parameter that can be used is the standard deviation of the logarithm of the volume, $\text{SD}(\ln V)$. The use of this function is rationalized by the fact that the volume distribution function is frequently of a log-normal character.

The point sampling intercept procedure proposed by Jensen and Gundersen [4] can be used to quantify the degree of grain volume uniformity. This is based on the equation that relates volume variance, $\text{VAR}_V(V)$, to the mean value of V :

$$\text{VAR}_V(V) = E_V(V^2) - (E_V(V))^2. \tag{3.2}$$

Jensen and Sorensen [5] have shown that:

$$E_V(V^2) = 4\pi k E(A^3). \tag{3.3}$$

In this relationship A is the area of the grains hit by the P_i points and k is a constant with a value in the range from 0.071 to 0.083. The value of k can be determined either experimentally or by appropriate modelling.

The above given analysis of the grain size diversity provides its an un-biased estimates. For simple ranking of grain structures one can also use coefficient of variation of grain section area, $CV(A)$ or intercept length, $CV(l)$.

4. Flow stress dependence on the distribution of grain size

The flow stress of polycrystals is known to be a function of the size of the grains, the properties of the grain interiors, and the nature of grain boundaries. It has been postulated almost 40 years ago that the flow stress is a linear function of $(S_V)^{-1/2}$:

$$\sigma = \sigma_0 + K(S_V)^{-\frac{1}{2}}. \quad (4.1)$$

A new consideration has been recently proposed taking into account the statistical nature of grain morphologies in polycrystals. This model consideration is based on the assumption that a polycrystal, described by a grain volume distribution function, $f(v)$, can be viewed as a composite of sub-polycrystals individually of constant size grains (CSG) so forming the polycrystal aggregate. The total volume of a sub-polycrystal v_{CS} built up of the grains of the volume v is given as:

$$v_{CS}(v) = N_T v f(v) dv \quad (4.2)$$

where N_T is the total number of grains in the polycrystal.

It is further assumed that the flow stress of CSG sub-polycrystals depends only on the size of grains through their volumes:

$$\sigma_{CSG} = g(v) = \sigma_0 + K_{CSG} v^{-\frac{1}{6}}. \quad (4.3)$$

where $g(v)$ is given by Eq.(1.1) with $d^{-1/2}$ being replaced by $v^{-1/6}$ (the mean diameter or the mean intercept length is proportional to the cube root of v). Such a dependence is rationalized by the existing models for the Hall-Petch relationship as it has been pointed out that they consider properties of the polycrystals to be characterized by a constant size of grains.

A polycrystal characterized by an overall diversity in the size of grains is viewed now as an aggregate of separate CSG sub-polycrystals. The flow stress of the polycrystal can be approximated by the following equation:

$$\sigma = \frac{1}{v_T} \int \sigma_{CSG} v_{CS} dv \quad (4.4)$$

where v_T stands for the total volume of the polycrystal specimen.

Integration for a log-normal distribution leads to the following modified version of the basic equation:

$$\sigma = \sigma_0 + K_{CSG} \exp[-a SD^2(\ln v)] d^{-\frac{1}{2}} \quad (4.5)$$

where:

- $SD(\ln v)$ – the standard deviation (SD) of the volume logarithm,
 K_{CSG} – the stress intensity constant of the Hall-Petch relationship for
 CSG polycrystals,
 σ_0 – the friction stress,
 a – a numerical constant.

In order to verify the modified formula for the grain size effect polycrystalline specimens were produced. The powder has been sieved in order to produce two fractions, subsequently mixed in different proportions to produce a series of different types of polycrystals. These polycrystals differed in the value of the ratio V_A/V_B specifying the relative volume (weight) of particles from fractions A and B. Binary images (after digitalization by automatic image analysis system) of the grain boundaries in the specimens are shown in Fig. 11.

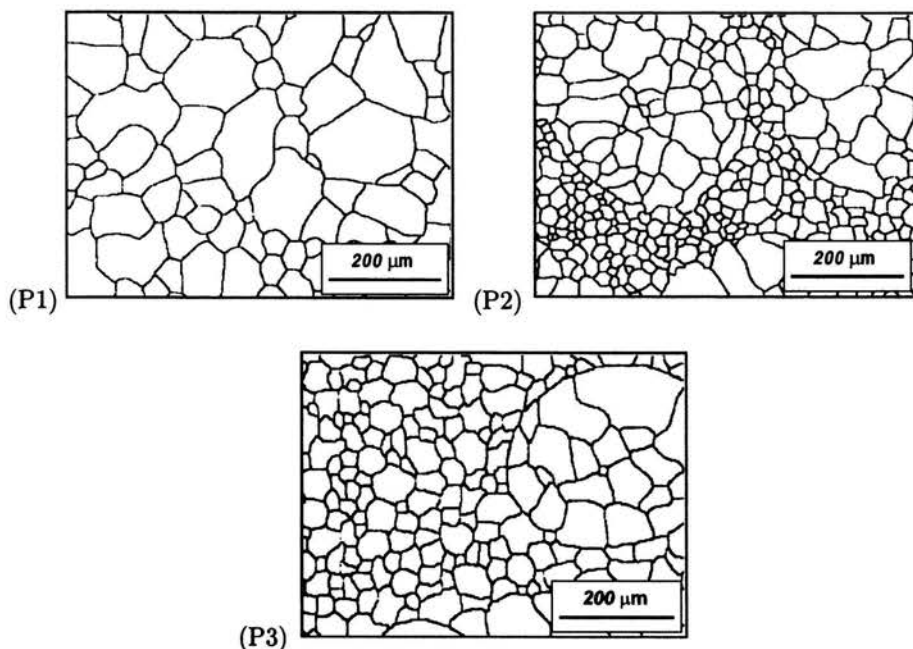


FIGURE 11. Images of the specimens showing systematically different homogeneity of the grain size.

Systematic measurements of the grain sizes were performed on the specimens using a system for automatic image analysis. The measurements included grain area A , and grain intercept length l . The mean values $E[A]$ and $E[l]$, and the coefficients of variations $CV[A]$ and $CV[l]$ as well as the normalized grain area distribution functions $f(A/E[A])$ for studied polycrystals P1, P2, P3 are depicted in Fig. 12.

Hardness measurements were used to characterize the mechanical properties of the material. In this case the Brinell hardness was measured at room temperature using a standard meter and metallographic microscope. For each specimen at least 15 indentations were made as this number was found to be sufficient for establishing stability of the mean values. In all cases a symmetric distribution of hardness

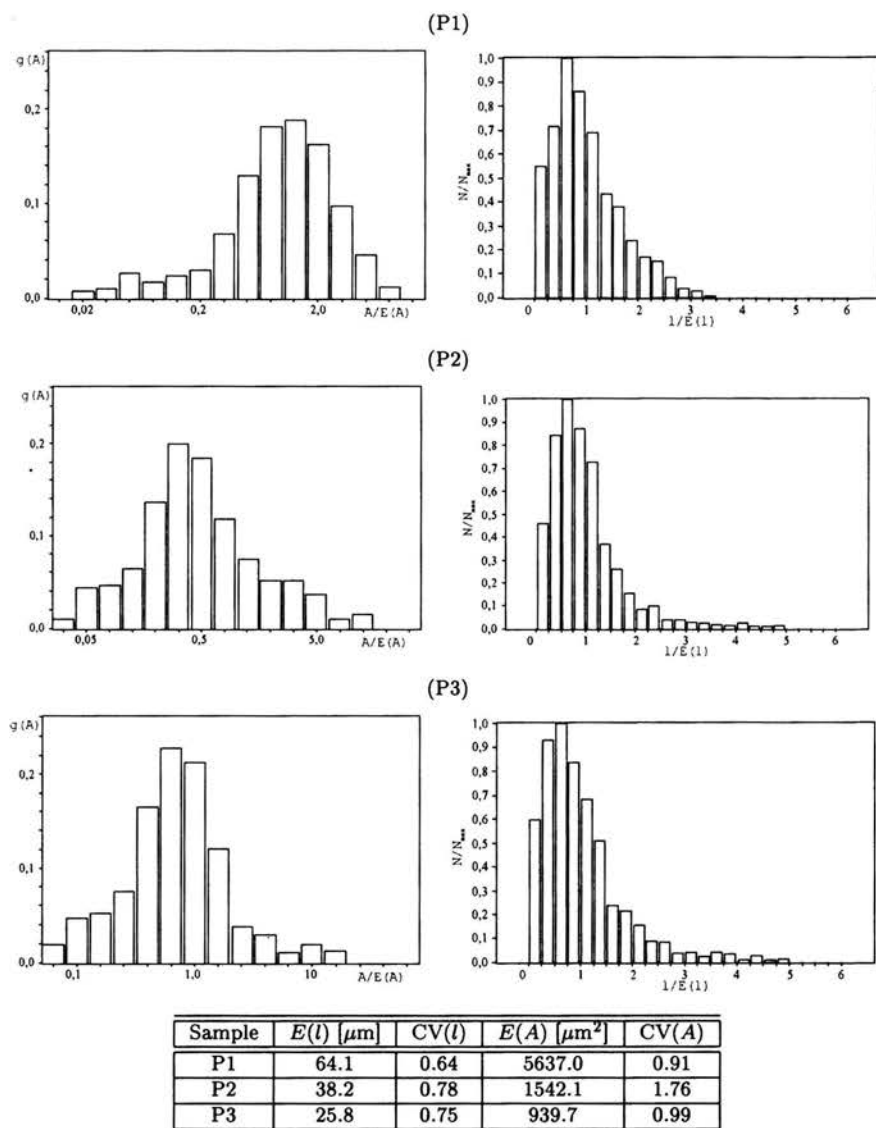


FIGURE 12. The distribution functions and the mean values of the grain section area for studied series of specimens.

values were observed. That permitted use of a *t*-Student distribution in finding 0.95 confidence intervals of the mean hardness values. The results of the measurements are given in Fig. 13.

Upon a closer examination of the experimental points it can be found that they systematically deviate from the lineal relationship predicted. Since the studied polycrystals were prepared from the same batch of powder and using the same technique

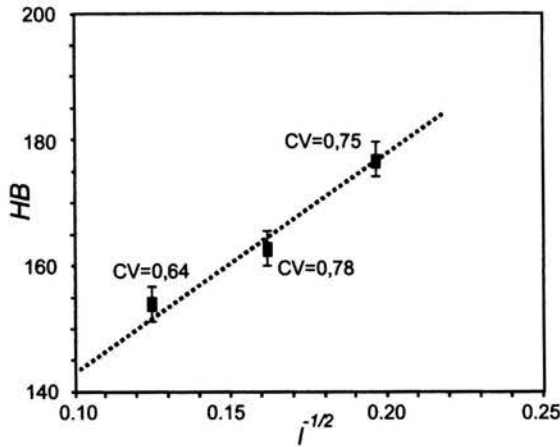


FIGURE 13. The results of hardness measurements.

and the same heat treatment the specimens studied differ mainly in the distributions of the size of grains. In this situation it can be concluded that the materials studied show a systematic deviation from Hall-Petch relationship in its classical form. Moreover, it can be concluded that the experimental points deviate from the linear relationship by the amount dependant on the variation in the normalized size of grains.

5. Quantitative stereology of particles

5.1. The geometry of particles

Particles are important 3D microstructural elements of a large number of materials. They are characteristic features of a large group of steels and metallic alloys, as well as of ceramics, composites and concretes which are formed either as a result of careful microstructural design (as for example precipitates in aluminum alloys) or due to shortcomings in manufacturing (as happens in the case of inclusions in some grades of steels).

In most cases these particles are present in the material to improve properties. For this function usually it is required that the particles are harder than the matrix in which they are embedded. Such particles contribute to a so called particle-strengthening effect. However, hard particles might also be sites of crack generation and a reason for a decrease in toughness of the material. As a result, particle-strengthening mechanisms can be used extensively only if the role of the particles is fully understood. This in turn requires precise information about their nature (chemical composition and microstructure) and a description of their geometrical features. The physical properties of particles in different materials are the remit of physical metallurgy, phase transformations and chemistry. In the present text, attention is focused on a description of their geometrical properties. This geometrical approach means that the solutions and methods presented here are of general

character and do not depend on the nature of the particles studied. The results can be applied to any system of particles; to nanometer size precipitates as well as to millimeter size inclusions in cast iron.

Some examples of microstructures containing particles are shown in Fig. 14.

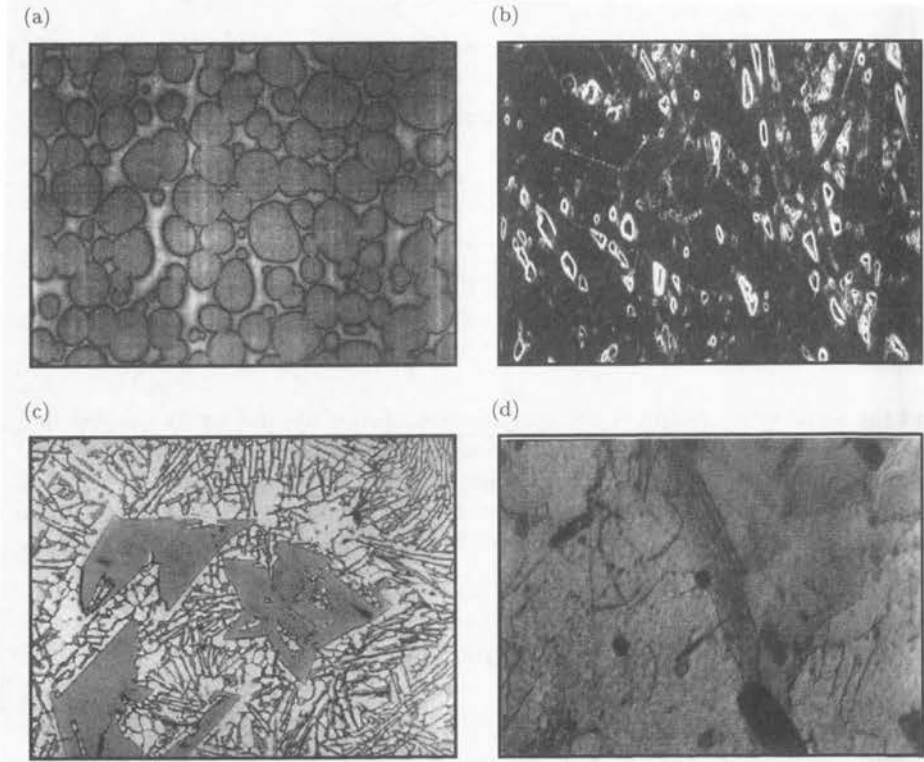


FIGURE 14. Images of particles in engineering materials:

- (a) tungsten particles in heavy alloys (SEM),
- (b) particles in ceramic-ceramic composite (SEM),
- (c) particles of Si in Si-Al alloys (optical microscopy),
- (d) carbides in Fe-Cr corrosion resistant alloy (TEM).

These examples illustrate important aspects of particles in materials: they differ among themselves in the details of their geometry. In other words particles form populations. A population in a given material consists of all particles V_1, V_2, \dots , or in shorthand notation V_i , with i ranging from 1 to N_T , the total number of particles.

A description of the geometrical features of the particles, in general, consists in characterizing their:

- content,
- shape,
- size,
- spatial distribution,

- location with respect to other defects,
- orientation.

Such a characterization can provide information on the whole system of particles without recognizing individual properties of the particles. This approach leads to such parameters as:

V_v – the volume fraction,

N_v – the mean density,

which are discussed in the subsequent part of the text.

5.2. Distribution functions

The individual parameters, X_i , implies the use of distribution functions, $f(X_i)$. These distribution functions provide information on the relative number of particles distinguished from the rest of the population by certain specific values of X . In materials science applications such a description might be simplified to include information on mean properties of the particles. The mean value, $E(X)$, is given by:

$$E(X) = \frac{1}{N_T}(X_1 + X_2 + \dots + X_{N_T}). \quad (5.1)$$

In this case the properties are averaged over all the particles in the material. This approach leads to parameters such as:

$E(V)$ – the mean volume,

$E(S)$ – the mean surface area.

In some cases a more detailed description is required which includes higher order parameters such as variation $\text{VAR}(X)$:

$$\text{VAR}(X) = \frac{1}{N_T} [(X_1 - E_X)^2 + \dots + (X_{N_T} - E_X)^2] \quad (5.2)$$

where $E_X = E(X)$. Alternatively the standard deviation:

$$\text{SD}(X) = \sqrt{\text{VAR}(X)} \quad (5.3)$$

or coefficient of variation:

$$\text{CV}(X) = \frac{\text{SD}(X)}{E(X)} \quad (5.4)$$

can also be used. These three parameters provide information on the variability in the property X of the particles. They are all equal to zero for a uniform population of particles in which all the elements show the same property ($X = \text{const.}$).

Measurements carried out on population of particles in a given material involve their sampling. Different sampling procedures are used in practice, which generate different descriptions of the material. In the case of point sampling with a 3-dimensional set of points of uniform density, the particles are sampled with a probability proportional to their volume, V_i . As a result particles with a larger volume are sampled more frequently than the smaller ones, even if they appear in equal

numbers per unit volume. This sampling with points generates volume-weighted estimates of microstructural parameters. These volume-weighted estimates of particle volumes, $E_V(V)$, are given as:

$$E_V(V) = \frac{1}{K} (V_1^h + V_2^h + \dots + V_K^h) = \frac{1}{N} \frac{(V_1^2 + V_2^2 + \dots + V_N^2)}{(V_1 + V_2 + \dots + V_N)} \quad (5.5)$$

where the summation is carried out over K particles hit by a grid of points.

In the case of probing with lines, the probability of hitting a given particle is proportional to its surface area, S_i . If a system of lines is drawn through a population of particles, a mean volume, $E_S(V)$, can be calculated by averaging the volume of particles hit by the lines:

$$E_S(V) = \frac{1}{K} (V_1^h + V_2^h + \dots + V_K^h) = \frac{1}{N} \frac{(S_1 V_1 + S_2 V_2 + \dots + S_N V_N)}{(S_1 + S_2 + \dots + S_N)} \quad (5.6)$$

On the other hand, it can be shown that random sections of the material reveal the particles with a probability proportional to their height h_i in the direction perpendicular to the section:

$$E_h(V) = \frac{1}{K} (V_1^h + V_2^h + \dots + V_K^h) = \frac{1}{N} \frac{(h_1 V_1 + h_2 V_2 + \dots + h_N V_N)}{(h_1 + h_2 + \dots + h_N)} \quad (5.7)$$

Distributed in the volume of a material, particles are sampled with the same probability regardless of their size and shape only in the case of volume sampling by means of a dissector. This procedure assumes that a slice of the material is cut which is bounded by two cross-sections and particles are accepted which do not emerge on one of the sections.

The particles sampled with the dissector yield a number mean volume:

$$E_N(V) = \frac{1}{N} (V_1 + V_2 + \dots + V_N) \quad (5.8)$$

A system of particles can be characterized generally in terms of their total volume, V , surface area, S , curvature, M , and number, N . These parameters depend on the geometry of the individual entities forming the population of the particles studied. However, this is a "one way" functional dependence, in the sense that for given values of V , S , M and N , there are different possible distribution functions of particle volumes, surface area etc. In the approach adopted in materials science, these quantities are usually referred to unit volume of the material. This is due to the fact that microstructure of materials is usually sufficiently homogenous to show volume-extensive properties. If referred to unit volume of a material these parameters define:

- the volume fraction, V_V ;
- the specific particle interface, S_V ;
- the particle density, N_V .

The volume fraction, $(V_V)_\alpha$, of α particles is one of the fundamental quantities used to characterize multi-phase materials. Its applications range from the theory of composite materials to phase transformations. The volume fraction defines the

fraction of the volume filled with particles. For a specimen of total volume, V_T , the volume fraction is defined as:

$$(V_V)_\alpha = \sum_{i=1}^N \frac{(V_i)_\alpha}{V_T} \tag{5.9}$$

where this summation is over all N particles in the volume of the specimen, V_T .

5.3. Cavalieri law

According to the basic stereological relationships, the volume fraction can be estimated by probing the microstructure with either sections, lines or points using the following set of equations (the Cavalieri law):

$$(V_V)_\alpha = (A_A)_\alpha = (L_L)_\alpha = (P_P)_\alpha \tag{5.10}$$

In these equations, the symbols have the following meanings: $(A_A)_\alpha$ is the area fraction occupied by particle sections on randomly cut cross-sections; $(L_L)_\alpha$ is the length of the intercepts inside particles as a fraction of the total length of random lines in 3 dimensions; $(P_P)_\alpha$ is the fraction of points hitting the particles from a system of points randomly distributed in space.

Application of these equations requires random sectioning of the specimens and either area measurements or further sampling with points or lines. In this context the term random can be replaced by systematic, assuming that all possible orientations are taken with the same probability.

There are two special situations that should be distinguished:

1. particles are isotropic;
2. particles are anisotropic, either in their orientation or distribution.

If the particles are isotropic, in principle all measurements can be performed on one representative cross-section of the material. However, it is strongly recommended to use more sections. Measurements on three mutually perpendicular

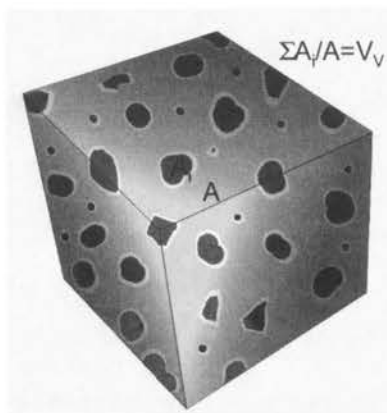


FIGURE 15. Estimation of the volume fraction of isotropic particles in ceramic matrix composite.

sections provide better estimates as well as an opportunity to test the isotropy of the particles (see Fig. 15).

The measurement of particle sections, A , can be made with the help of an image analysis system. The same applies to measurements of intercept length (the intercept lines may form a grid of lines parallel to a given direction). On the other hand, simple counting can be carried out if a grid of points is used, although this again can be effected using an image analysis system. It should be noted that the precision of estimation by point counting is not worse than the other two methods.

If the particles are anisotropic, the sections should be random in 3-dimensions. Random in this case means random in position and in the orientation of the vector normal, \mathbf{n} , to the cross-sections taken. This might be difficult to implement and as an alternative vertical sections can be made, see Fig. 16.

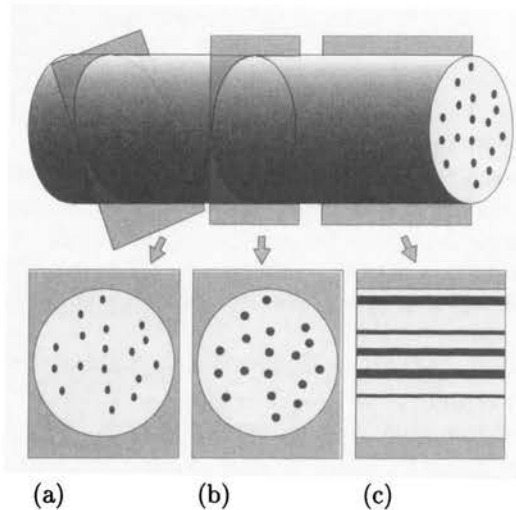


FIGURE 16. Random (a), parallel (b) and vertical (c) sections of a two-phase material.

5.4. Specific surface area estimation

Specific interface/surface area, or in other words, surface-to-volume ratio, S_V , is another elementary parameter which describes some properties of a system of particles. It can be used generally in any studies related to interfacial phenomena such as:

- phase transformations;
- particle growth;
- interfacial cracking.

In its basic form, it defines the total area of the surface separating particles from the matrix in which they are embedded. Based on the results of stereology, this parameter can be estimated using a system of random lines in 3-dimensions. If such lines are drawn throughout the volume, V_o , and hit N_l particles per unit length, the total particle surface area can be estimated from the relationship:

$$S = 4N_l V_o. \quad (5.11)$$

This equation can be transformed further into the following relation:

$$S_V = 4N_L = 2P_L \quad (5.12)$$

where P_L is the density of intersection points of the 3D random test line array with the interphase boundaries of the particles studied.

Implementation of this formula depends again on the isotropy/anisotropy of particles. If they are isotropic, the lines can be drawn on any section and sets of parallel lines can be used.

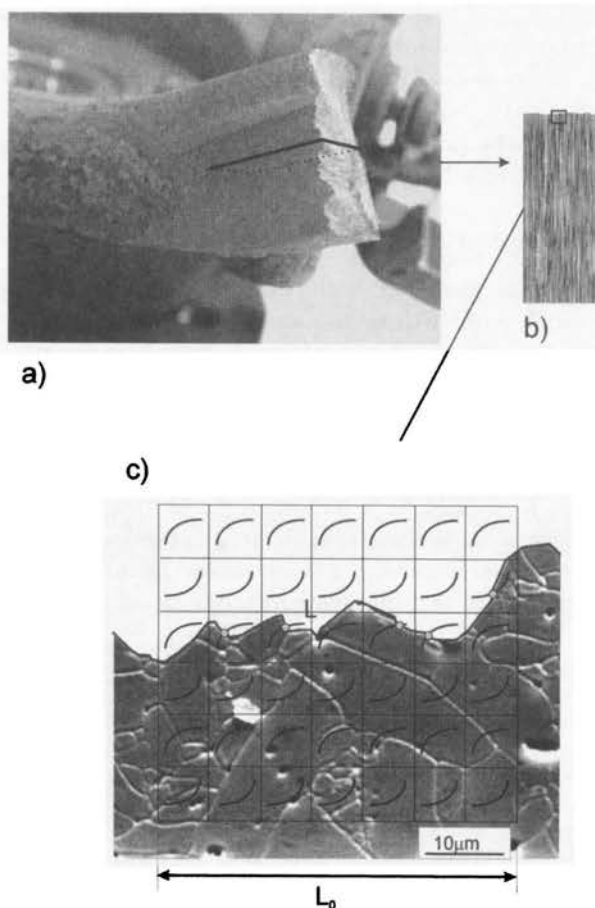


FIGURE 17. Explanation of the method of vertical sectioning:
 (a) the specimen,
 (b) vertical sections,
 (c) images and measurements using test lines in form of cycloids.

If the particles are anisotropic, or the isotropy cannot be taken for granted, the test lines need to be randomly oriented in space and more sophisticated methods have to be employed to draw such a system of lines. One of the solutions offers, in this case, the method of vertical sectioning explained in Fig. 17.

The number of intersection points with cycloids, I_j , is determined for each vertical section cut, C_j . Also the fraction of testing points, P_i , falling into the reference space is counted. An estimator of S_V , defined as the ratio S to the volume V of the reference space is given as follows:

$$S_V \approx 2 \frac{M}{\sum P_i} \frac{\sum I_j}{L} \quad (5.13)$$

where M is the final magnification of the microstructural images and L is the total length of the cycloids used.

The intersection points from a grid of cycloids can be counted with respect to the area of the material examined on a particular cross-section. In this case, the reference space is the volume of material and in most practical cases $P_i = 1$, which means that all the testing points are within the image of the microstructure. The reference space can also be the volume of the particles studied and then P_i describes the volume fraction occupied by the particles.

5.5. Density of particles

According to stereological notation the density of particles is designated by N_V . This defines the number of particles in a given reference volume, V . In the case of materials in which particles are distributed more or less uniformly, this parameter defines the number of particles in a unit volume.

Despite its apparent simplicity, the methods of N_V estimation are not quite obvious and for years were the object of intensive theoretical studies. This difficulty was related to the lack of proper sampling procedures for particles distributed in space. The most frequently used technique for particle observations is an examination of 2-dimensional sections. From the point-of-view of stereology this is equivalent to sampling particles with a plane probe. In this case a plane is drawn through the system studied and observations are made of the particles hit by this

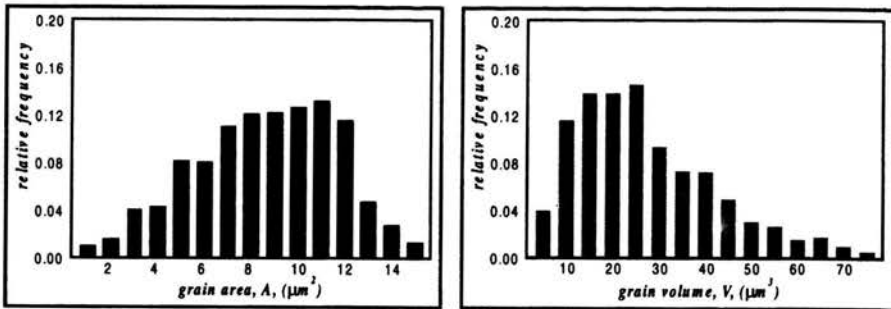


FIGURE 18. Illustration of the size effect on the probability of revealing particles in images of the materials microstructures.

plane. However, this manner of particle selection introduces a systematic error due to the fact that large particles are hit more frequently than the smaller ones as illustrated schematically in Fig. 18. In fact the particles are sampled (hit by the plane) with a probability proportional to their height, h_i . With such a sampling procedure, whatever measurements are made, there is a likelihood of introducing a bias.

This problem of particle sampling was resolved in the past by making assumptions with regard to the particle shape. Actually, in order to obtain reliable results, it was necessary to describe beforehand the shape of particles quite precisely. Simple solutions have been obtained for features which have shapes such as spheres, rods, disks and ellipsoids.

The classical procedure starts from the assumption that we deal with a system (material) containing particles of a known shape, for example in the form of cubes. It is also assumed that the particles have sizes, measured for example by volume or edge length, in the present case designated as L , varying from 0 to some maximum value L_{\max} . This range of sizes is divided into a finite number of classes, L_i , where $i = 1, 2, 3 \dots N$. The relative number of particles in each class is designated N_i .

Knowing the shape of particles, it is possible for each size class to obtain theoretical distributions of particle sections. This can be done either experimentally, by studying 3D model figures, or with the help of computer simulations. Usually the analysis starts with the largest particles in the class L_N , i.e. the range of particle sections is obtained from 0 to some maximum section size, A_{\max} . This range of particle section sizes is divided into M classes, A_j ($j = 1, 2 \dots M$), with the biggest sections in class A_M . In the next step the relative numbers of sections in each class, n_{jN} , are established for the particles in class L_N . By proceeding to the classes of smaller particle size, a matrix is obtained, n_{jK} , which defines potential contributions of particles of size K to the sections of size j .

The next part of the procedure is to produce a model of the experimental process of particle sampling or, in other words, a decision is made as to what are the chances of revealing on the cross-section particles of a given size. In most cases, the chances of cutting a particle are proportional to its height and in the case of cubes it is proportional also to the length of the edge. This means that particles with an edge length 10 times larger are 10 times more frequently cut by the section of observation. In this way the expected relative number of sections in a given class can be expressed in the following way:

$$n_j = N_1 L_1 n_{j1} + N_2 L_2 n_{j2} + \dots + N_N L_N n_{jN}. \quad (5.14)$$

This is a linear equation that can be solved to find one solution if $N = m$.

A number of shapes has been analyzed in detail and a comprehensive summary is given in [1]. The analysis due to Underwood [1] covers both regular spheres as well as elongated particles. For the case of particles with fixed shape and size the general formula can be simplified to:

$$N_V = \kappa \frac{N_A^2}{N_L} \quad (5.15)$$

with the value of κ dependent on the projected area and height of the particles. The values of κ for selected particle shapes are given in Fig. 19.






shape					
κ	$\pi/4$	$2/\pi$	$2/3$	0.732	0.756

FIGURE 19. Simple shapes of particles and respective values of κ parameter.

For the case of a system characterized by a particle size distribution function the above equation needs to be modified and additional parameters have to be measured. For a system of spherical particles of different sizes this additional parameter is m – the mean value of the reciprocal of the particles' cross-section diameter d_i :

$$E(m) = \frac{1}{N} \sum_{i=1}^N \frac{1}{d_i}. \quad (5.16)$$

The differences in the analysis between constant size and variable-size systems of particles are demonstrated for the microstructures shown in Fig. 20.

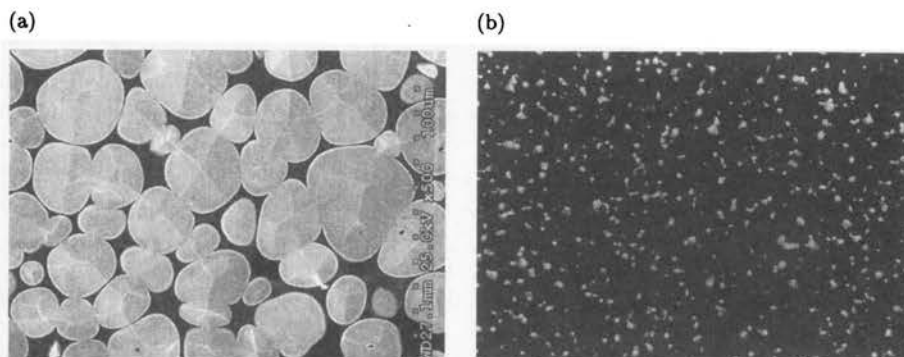


FIGURE 20. Image of particles in a two-phase material and estimation of the their density.

The mean volume of particles can be approached either with some specific assumptions about their shape or without such assumptions at the expense of making more sophisticated measurements. If the first method is chosen, one has to follow the procedures already described, based on the division of the particles of a model shape into size classes. The focus of the discussion which follows is therefore to be placed on the assumption – free techniques. The discussion starts with the description of the method for the determination of the mean particle size and the coefficient of its variation, and then moves to an estimation of the size distribution function.

5.6. Spatial distribution of the particles

Spatial distribution of the particles can be quantitatively described using the method of covariance and tessellation.

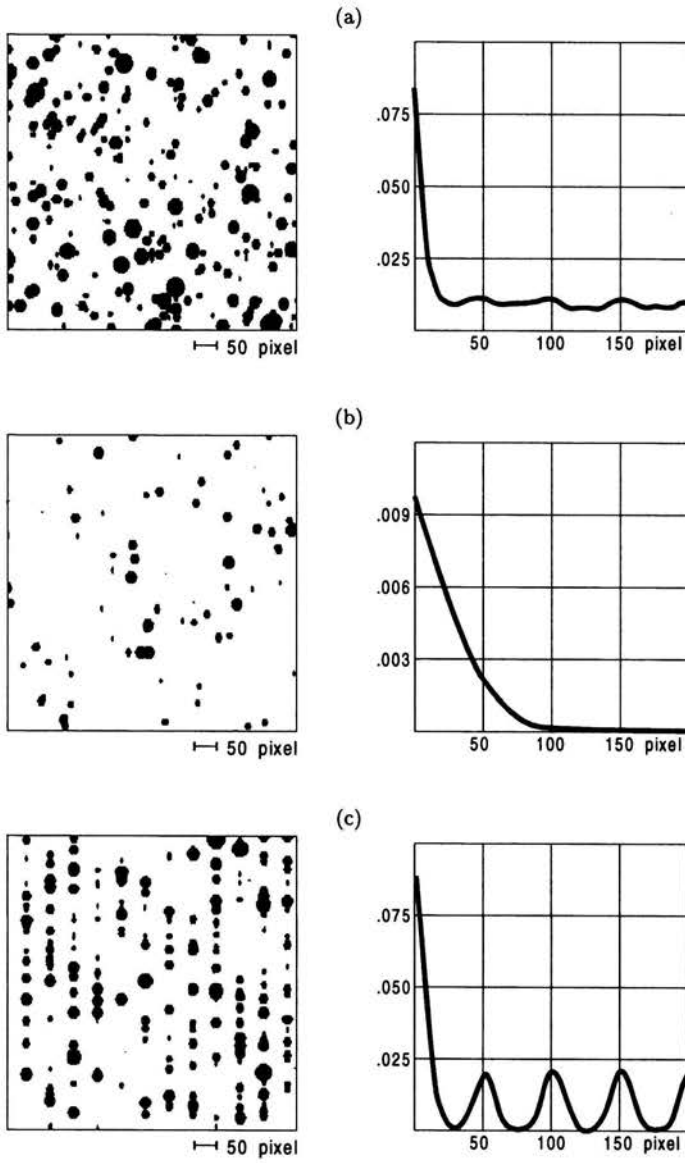


FIGURE 21. Plots of the covariance function for: (a) random, (b) clustered and (c) periodic structures.

The covariance function defines, for a given distance r , the probability, $P = C(r)$, that two points are at a distance r apart and both hit the features of interest:

$$C(r) = P[(x \text{ hits a particle}) \wedge ((x + r) \text{ hits a particle})]. \quad (5.17)$$

For a homogeneous and isotropic system of features the covariance depends only on the distance r and is independent of the position of the test points in space. For a random distribution of particles $C(r)$ does not depend on r .

The examples of the covariance function for different types of structures are shown in Fig. 21.

In case of random structure (Fig. 21a) the covariance function drops rapidly to certain value, depending on the volume fraction of particles and remains close to it with only stochastic fluctuations. In the case of the clustered structure (Fig. 21b) the situation is quite similar, except that the initial decrease is less rapid than in the case of random structure. For the periodic structure (Fig. 21c) the covariance function measured in proper direction reflects well the periodic nature of analyzed sample.

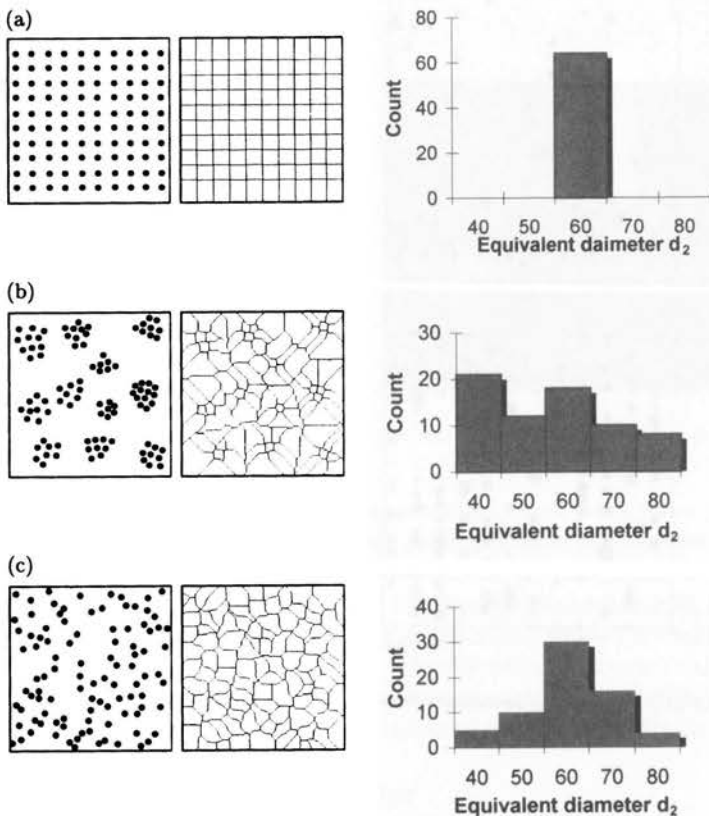


FIGURE 22. The zone of influence of a given particle for: (a) periodic, (b) clustered and (c) random structures with corresponding histograms of the zone size distribution.

For a homogeneous and isotropic system of features, the covariance depends only on the distance r and is independent of the position of the test points in space. For a random distribution of particles $C(r)$ does not depend on r .

Tessellation method is based on the computer-aided technique of image processing known as SKIZ (skeleton by influence zone). This method transforms a system of points into granular structures, such as those shown in Fig. 22. Each of the grains of the structure constitutes the zone of influence of a given particle, i.e. a set of points whose distance from this particle is smaller than its distance from any other particle.

The structure thus generated is subjected to a standard quantitative analysis, in which we determine the distributions of grain sizes and shapes (influence zones), among other quantities. For each distribution obtained, we can subsequently determine several statistical values, such as the average, standard deviation, variation coefficient etc., which together form the characteristic of the particle distribution in a given structure.

5.7. Particle shape characterization

Particle shape is a much more complicated property than size. This is especially evident when attempts are made to quantify the shape by means of some number of parameters. As a result, in many cases the shape of objects is described by a sketch or illustrated in a series of images taken from different angles of observation without any attempt to transform them into a formal mathematical description. Thus, particles are merely classified into some broad categories represented by a conventional geometrical object. The following categories of particle are frequently distinguished:

- spheres;
- cubes;
- disks;
- needles;
- plates.

The first two from this list, i.e. spheres and cubes, have their shape uniquely defined and do not need further specification. This is not true for the next three. The shape of disks can be more precisely described by the ratio of their thickness t , to the radius of the maximum section R :

$$\frac{t}{R} \quad (\text{disks}).$$

The shape of needles on the other hand depends on the ratio of the needle length l , to the maximum radius r in the direction normal to the elongation axis:

$$\frac{l}{r} \quad (\text{needles}).$$

The shape of plates can be differentiated in terms of the ratio of the true surface area S to the projected surface area in the direction approximately normal to the plate S_p :

$$\frac{S}{S_p} \quad (\text{plates}).$$

This list is far from being complete and more geometrical objects can be studied and described in terms of some simple dimensionless parameters.

Particle shape can also be described in terms of geometrical properties such as number of faces F , number of edges E , etc. In this case a cube exemplifies a shape which is coded as $F = 6$ and $E = 12$. On the other hand a spherical particle is described by $F = 1$ and $E = 0$.

From the point-of-view of materials science, important geometrical properties are those which describe:

- the degree of elongation,
- the degree of surface complexity.

The importance of information on the possible elongation of particles is related to the potential anisotropy of the material properties. The degree of surface complexity is important in analyses of phenomena taking place at interphase boundaries, such as segregation and phase transformations. These properties, elongation and surface complexity, can be quantified by means of the following ratio:

$$\frac{R_S}{R_V}$$

where R_S and R_V are equivalent surface and equivalent volume radii respectively, i.e.:

$$R_S = \sqrt{\frac{S}{4\pi}} \quad (5.18)$$

and

$$R_V = \sqrt[3]{\frac{3V}{4\pi}}. \quad (5.19)$$

One can also use the ratio of R_S^c to R_S , R_S^c/R_S , where R_S^c is the surface radius of the minimum volume sphere that contains the volume of a given particle. The values of the ratios defined in this way are given in Fig. 23 for some simple geometrical forms.

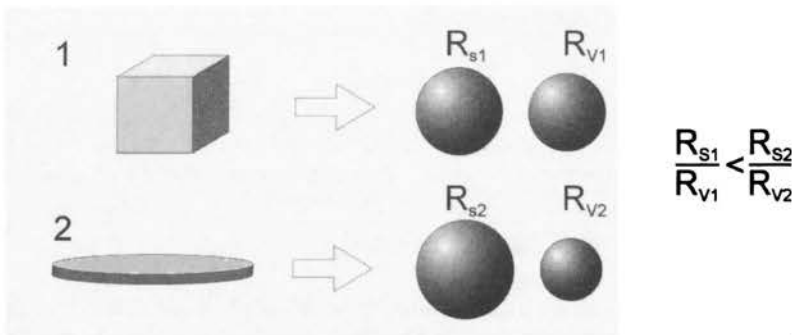


FIGURE 23. Examples of simple particle shapes and respective values of shape factors.

Another approach to particle shape concentrates attention on the properties of the system instead of looking at the geometry of individual elements. The degree of particle convexity can be described using the concept of the so called star volume, V^* . This star volume is the volume of the portion of space inside a particle which is directly seen from a point inside the particle, for example its center of gravity. For convex particles the star volume V^* is the same as the true volume:

$$V^* = V.$$

On the other hand for concave particles:

$$V^* < V.$$

The ratio of the mean values of the two parameters, V^*/V , is therefore a measure of particle convexity.

The method for estimation of the mean weighted particle volume based on point sampled intercepts has been described in the preceding sections of this chapter. The mean volume-weighted particle star volume, $E_V(V^*)$, can be estimated using the same procedure, if only those intercepts are taken which end at the sampled point. The costar coefficient can be used which is defined as follows:

$$\text{costar} = \frac{E_V(V) - E_V(V^*)}{E_V(V)}. \quad (5.20)$$

This coefficient is equal to 0 for convex particles and it increases with an increasing degree of irregularity in the shape of particles. The upper limit of the costar is equal to 1.

6. Examples of applications

6.1. Nano-intermetallic processed via severe plastic deformation

The benefits of using modern methods of description of microstructures are demonstrated here for nano-intermetallic processed via severe plastic deformation, SPD. A representative image of the microstructure of the material in question is shown in Fig. 24. The results of grain size and shape measurements are given in Table 2.

TABLE 2. Results of the stereological measurements carried out on the images of SPD processes nano-polycrystals of Ni_3Al .

Parameter	S_V [1/nm]	N_V [1/nm ³]	$E(V)$ [nm ³]	$E_V(V)$ [nm ³]	$E(d_3)$ [nm]	$E(d_{\max}/d_2)$	$E(p/\pi d_2)$
Values	0.04	$8.6 \cdot 10^{-6}$	$1.17 \cdot 10^5$	$1.24 \cdot 10^5$	44.3	1.42	1.30

The results of the measurements carried out on the images of the nano-material referred to in the present paper show can be compared with the values of the

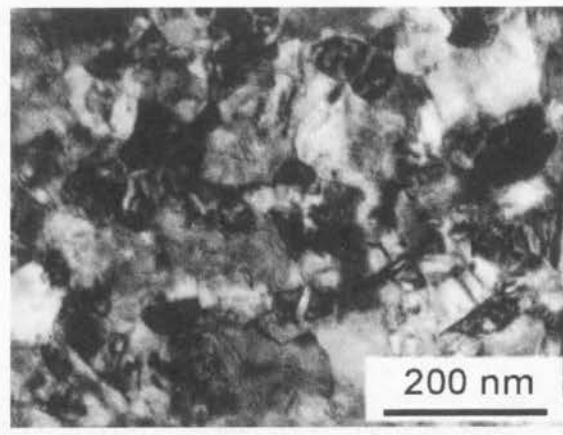


FIGURE 24. The structure of the nanointermetallic (Ni_3Al) processed via severe plastic deformation.

same parameters determined for micro-sized polycrystals. On that basis it can be concluded that the studied nano-polycrystals exhibit significantly higher values of the shape factors being used as a measure of the grain elongation (d_{\max}/d_2), and as the measure of the waviness of the grain boundary ($p/\pi d_2$). This finding implies, in turn, that the geometry of grain boundaries in such materials exhibit a non-equilibrium geometry. As a result, any process of equilibration of grain boundaries in this material should involve both equilibration of the microstructure and geometry of the grain boundaries.

6.2. Distribution of carbon particles in SiC based ceramic composite

The application of the covariance method have been demonstrated in the study of the carbon distribution in SiC based ceramic composite. The images of the carbon particles (white) in SiC matrix are shown in Fig. 25.

The results of the studies of the carbon particles distribution in SiC based ceramic composite are shown in Fig. 26. It has been found that the particles of carbon exhibit a tendency to clustering only for low level of carbon. This tendency is indicated by the position of the covariance function with respect to the reference curves: $C(r)_{\text{ref}} = V_V^2$, which are expected for a system with randomly distributed particles.

6.3. The effect of the contiguity in tungsten heavy alloys

The effect of particle contiguity on toughness have been studied on typical tungsten heavy alloy (WHA). The alloys studied have been fabricated from powder mixtures by a liquid phase sintering at about $1450\div 1500^\circ\text{C}$. After sintering the composite consists of a contiguous network of nearly spherical tungsten particles embedded in a Fe-Ni-W ductile matrix (Fig. 27).

The mechanical properties of heavy alloys are primarily linked to the strength of W-matrix interface and the relative fraction of W-W interfaces, which are the

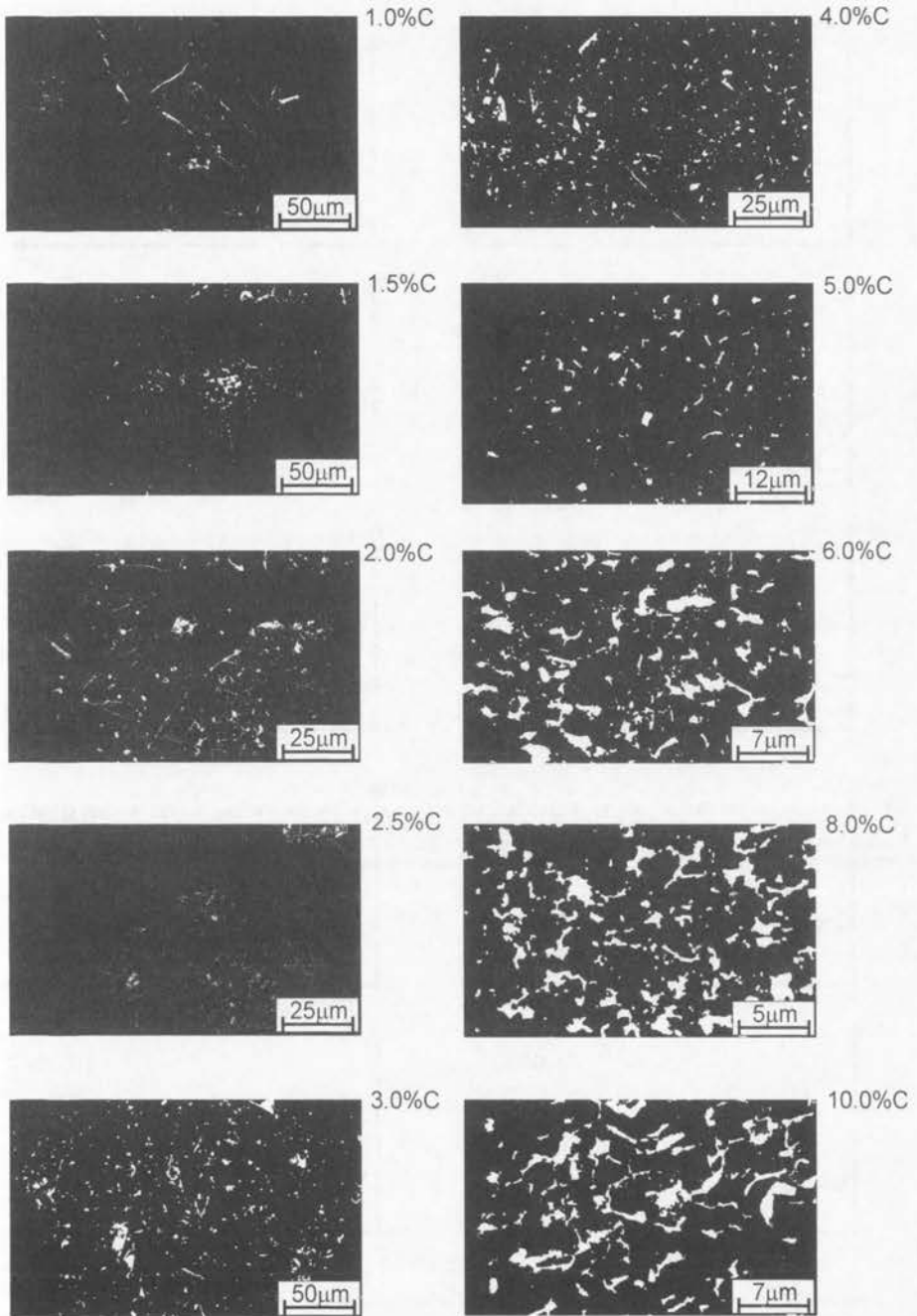


FIGURE 25. The images of the carbon particles (white) in SiC matrix with different carbon content.

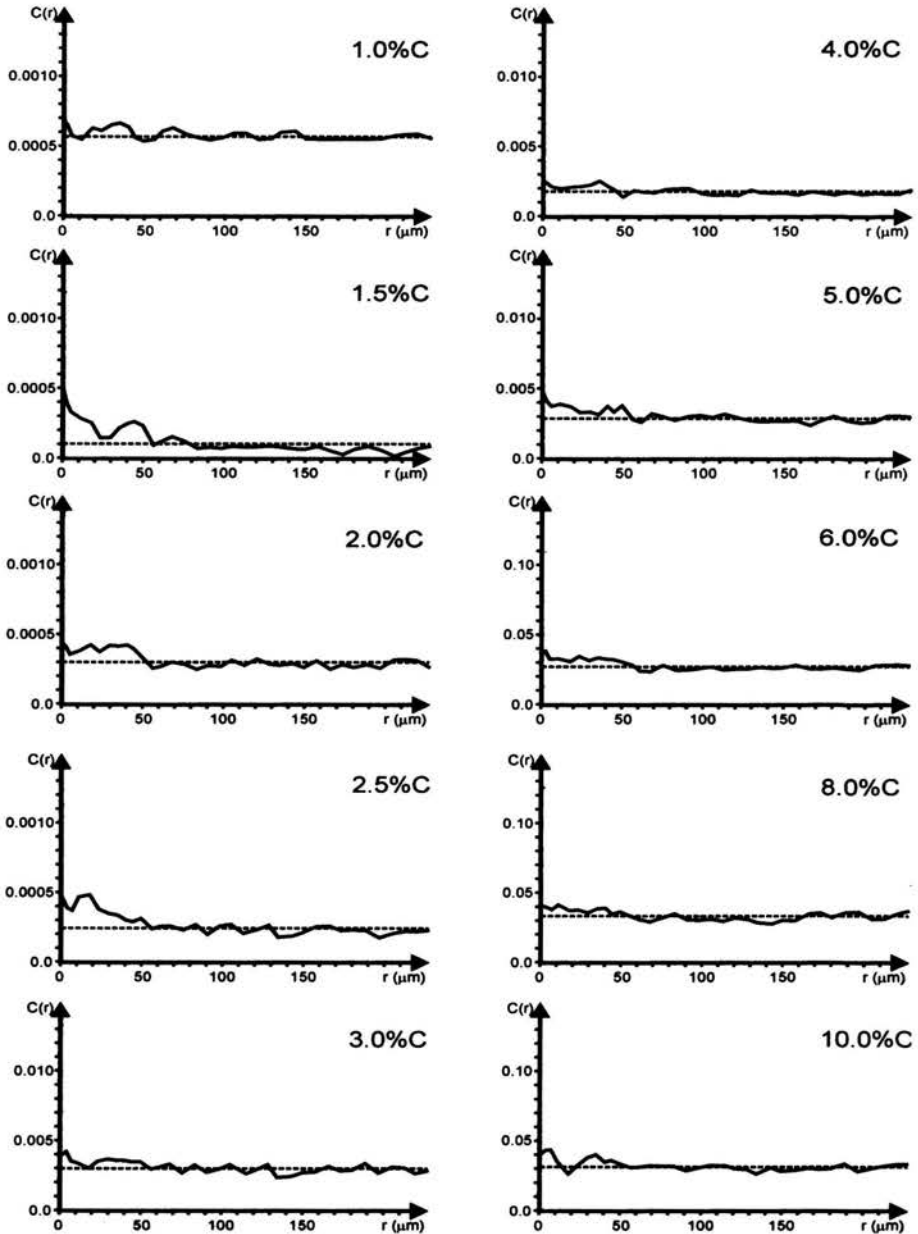


FIGURE 26. Plot of the estimated values of the covariance function, $C(r)$, for the studied samples. The respective reference lines (dashed) are computed for the measured value fractions of carbide particles.

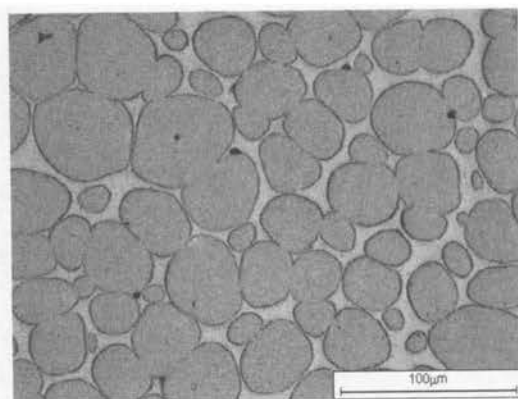


FIGURE 27. Typical micrograph of WHA studied.

weakest microstructural element of the alloy. The contiguity parameter C , defined as the fraction of W-W interfacial area in total area of interfaces in a volume of an alloy, can be provided as structural parameter which may well correlate with mechanical properties. Values of C parameter can also be correlated with other microstructural characteristics. Such a correlation is useful for property control and designing of WHA.

The images of the microstructure were digitised. Measurements of W-W interfaces were carried out using a concept of vertical sectioning and system of cycloid test lines. In order to calculate contiguity value, C , pairs of images were used: image A showing all W-matrix interfaces and image B with only W-W interfaces (or all interfaces).

The C values were counted using the following equation:

$$C = \frac{2N_{p_{W-W}}}{N_{p_{W-M}} + 2N_{p_{W-W}}} = \frac{2S_{V_{W-W}}}{S_{V_{W-M}} + 2S_{V_{W-W}}} \quad (6.1)$$

where:

- $N_{p_{W-W}}$ – the number of W-W grain boundary interceptions with cycloid lines,
- $N_{p_{W-M}}$ – the number of W-matrix grain boundary interceptions with cycloid lines,
- $S_{V_{W-W}}$ – the surface area of W-W grain interfaces per unit volume,
- $S_{V_{W-M}}$ – the surface area of W-matrix interfaces per unit volume.

Data obtained from the image analyses, microhardness measurements and the impact tests are summarised in Table 3.

A quantitative comparison of microstructures shows that particle size in all groups of cold worked samples is similar. As expected, the total tungsten grains surface area per unit volume is notably higher for samples with the small particle size, also contiguity is correlated with particle size (Fig. 28).

There are four potential fracture paths, that can be defined for the WHA: through the matrix, across tungsten particles, along tungsten-tungsten interfaces and tungsten-matrix separation. The W-W boundaries are the easiest fracture path.

TABLE 3. Data obtained from the measurements of microstructural features, impact strength and microhardness.

Specimens	$E(d_2)$ [μm]	S_V [1/mm]	C	Impact strength [J/cm ²]	Microhardness HV0.05	
					grains	matrix
As-sintered	27.1	81.6	0.23	184	404	295
Swaged	16.5	115.8	0.36	72.5	478	351
Rolled	18.3	109.0	0.34	10	557	360
Hydroextruded	18.6	110	0.33	34	574	373

Microstructural characteristic data was obtained from the longitudinal sections.

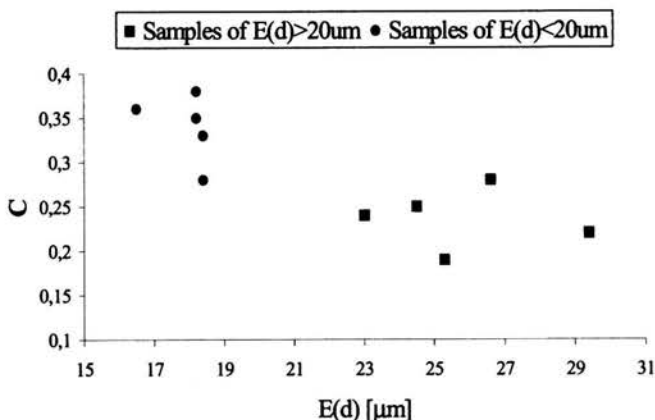


FIGURE 28. The plot of the contiguity vs. grain size for WHA studied.

The cracks at these boundaries were observed even in samples subjected to a small amount of cold working (before impact tests). Tungsten cleavage is observed at sufficiently high stresses, for which good W-M interfacial bonding is needed. The poor intergranular strength can be associated with an interface segregation or precipitation at the boundaries during sintering or during post sintering heat treatment. This reduces the load which can be carried out and reduces ductility of the material in a proportion depending on the contiguity.

Results obtained from the contiguity measurements give better insight to the fracture resistance of WHA. The contiguity varies in a broad range and is correlated with the tungsten particle size. For small particles ($E(d) = 16.5\text{-}18.7 \mu\text{m}$) C is relatively high ($C = 0.28\text{-}0.38$). For samples of large size ($E(d) = 23.0\text{-}29.4 \mu\text{m}$) C is smaller ($0.20\text{-}0.28$).

6.4. The microstructure of Al-Si alloys and Si particles distribution

Properties of Al-Si alloys depend on chemical composition and their microstructures. In particular, size, shape and orientation of Si particles influence their resistance to the plastic deformation and fatigue. The specimens used in the present work, designated as AS12, AS12V, AS12TT and AS13, AS13 TT were obtained

at Ecole de Mines in St. Etienne (France) using the following processing routes: AS12V – one step casting in vacuum, AS12 and AS13 – an original solidification process, AS12TT – obtained from AS12 via an additional annealing at 565°C for 12 h (to equilibrate geometry of Si particles), AS13TT – obtained from AS13 via an additional annealing at 515°C for 8 hours (to change the shape of FeSiAl₅ particles).

Microstructures of the specimens of the materials have been studied on randomly selected sections oriented parallel to their axis. The sections of the specimens were polished and images of Si particles were obtained using an X-ray microprobe mapping.

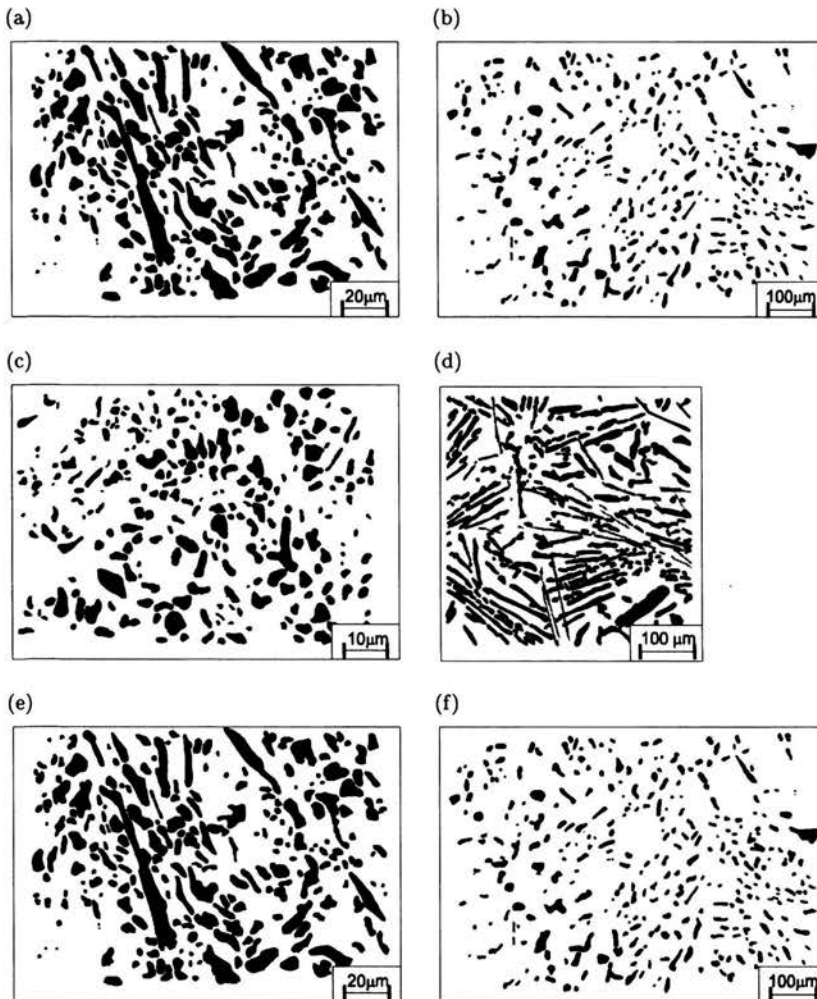


FIGURE 29. Binary images of Si particle revealed on the sections of the studied alloys: (a) AS12; (b) AS12TT; (c) AS12V; (d) AS13 (the initial images were obtained by X-ray microprobe mapping).

The micrographs have been digitized and transformed into to binary (black and white) images by a proper filtering and threshold operation. Microstructures typical of the studied alloys are shown in Fig. 29. In these images the silicon particles are unveiled as black isolated areas and Al-Si eutectic as a white matrix.

The following parameters were used to characterize geometrical features of a system of Si particles: the volume fraction, V_V , and specific surface area of interface between Si and the matrix per unit volume, S_V .

The microstructural parameters used here included also specific dimensions of individual sections of Si particles. To this end the following parameters were used: the circle equivalent diameter, d_2 , and the length maximum chord, d_{\max} . These two parameters, measured for each section by image analyzer, were subsequently used to determine section shape factor, d_{\max}/d_2 , which is a sensitive measure of particle elongation. It is equal to 1 for circles and its value increases with increasing elongation of the particles. The relative particle section elongation $\Lambda = (d_{\max} - d_2)/d_2$ was also calculated which is equal to zero for circles.

The parameters measured for Si sections were analyzed in terms of their mean values, designated as $E()$, standard deviations, SD, and coefficients of variation, CV, ($CV = SD/E$).

The quantitative description included also spatial orientation of Si particles. To this end the angle ω was determined between the orientation of the maximum chord of each particle section and the specimen axis. For each value of ω a shape factor weighted number of particle sections, N_ω , characterized by the orientation of d_{\max} within the interval of $(\omega - 3^\circ, \omega + 3^\circ)$ was computed. The N_ω parameter is defined either as:

$$N_\omega = \sum \left(\frac{d_{\max}}{d_2} \right) \quad \text{or} \quad N_\omega^* = \sum \left(\frac{d_{\max}}{d_2} - 1 \right) \quad (6.2)$$

with the summation being carried out over the sections with d_{\max} direction within $\pm 3^\circ$ from ω in both cases. Such definitions of N_ω makes this parameter sensitive to the orientation of elongated sections. It can be noted that N_ω is equal to 1 and $N_\omega^* = 0$ for circles. These weighted numbers of particles were analyzed as function of ω using a rose type plots.






Results of the measurements are listed in Table 4.

It can be noted that the studied microstructure differ significantly in terms of the size and shape of Si particles. The volume fraction of the particles, V_V , varies in the range $18.8 \div 21.0$ while the surface area of the interfaces alters from 120 to 590 μm^2 in the cubic micron ($1 \mu\text{m}^3$). The mean values of d_2 vary from 2 to 13 microns.

The histogram of d_{\max} are shown in Fig. 30. This parameter is of special interest here because Si crystals act on a micro-scale as stress concentrators and fatigue cracks in studied materials were observed at interfaces between Si particles and the matrix. It can be noted that the AS12V alloy is characterized by the presence of small size Si particles for which maximum chord, d_{\max} , does not exceed $10 \mu\text{m}$. The particles of such a size are also predominant in the microstructure of AS12. However, in this alloy d_{\max} reaches values up to $100 \mu\text{m}$. The microstructure of AS13 is much coarser, with mean values of d_{\max} close to 30 and maximum values above $100 \mu\text{m}$.

The quantification of the shape of Si particles in the studied materials reveals a considerable elongation of their sections. The mean value of the shape

TABLE 4. Geometrical characteristics of sections of Si particles in terms of the mean values, coefficients of variation of maximum chord, equivalent diameter and using representative ellipses.

Alloy	$E(d_2)$ [μm]	$CV(d_2)$	$E(d_{\text{max}})$ [μm]	$E\left(\frac{d_{\text{max}}}{d_2}\right)$	$\Lambda = \frac{E(d_{\text{max}} - d_2)}{E(d_2)}$	V_V	S_v [1/ μm]	$E\left(\frac{d_{\text{max}}}{d_2}\right)$	Representative ellipses
AS12V	2.0	0.5	2.7	1.34	0.35	18,0	589	1.34	
AS12	4.5	0.6	7.0	1.41	0.56	21,0	292	1.37	
AS12 TT	12.7	0.4	18.3	1.37	0.44	17,0	56	1.41	
AS13	9.9	0.4	23.4	2.22	1.36	15.8	153	2.01	
AS13 TT	12.5	0.4	27.2	2.01	1.18	16,8	121	2.22	

factor, $E(d_{\max}/d_2)$ reaches the lowest value for AS12V. In the case of this alloy $E(d_{\max}/d_2) = 1.34$ and this is close to the mean values for grain sections in well annealed polycrystals. The highest values of $E(d_{\max}/d_2)$ were obtained for AS13 and AS13TT.

It can be also noted that the heat treatment applied to AS12 results in a measurable changes in the shape of particles which become less elongated. This change in geometry is reflected by a decrease in mean value of d_{\max}/d_2 and S_V . In the case of AS13 the effect of the additional annealing is much less pronounced. The histogram in Fig. 30 indicates that this treatment lowers fraction of particles between 80 and 100 microns.

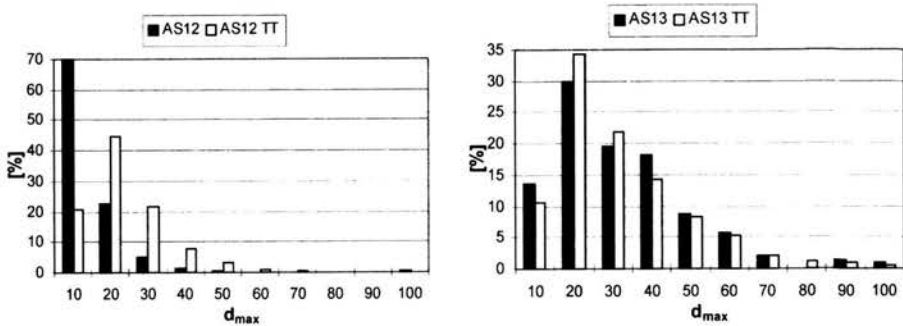


FIGURE 30. Histograms of the maximum chord, d_{\max} , for the specimens of: (a) AS12 and AS12T, (b) AS13 and AS13TT.

The results of the study of particle spatial orientation are presented in Fig. 31. The results show that in AS12V orientation of particles is isotropic. On the other hand in AS12 the majority of Si particles are oriented at an angle of $45^\circ \pm 15^\circ$ to the specimen axis. A considerable number of particles are also aligned parallel to the direction of solidification. The additional heat treatment applied to AS12 leads to the re-orientation of Si particles predominantly along the directions close to $\pm 45^\circ$ and to 90° . In the case of AS13 the preferential orientations are $-30^\circ \pm 15^\circ$ and 90° . However, other orientations, including parallel to the sample axis, are also observed. The heat treatment leads to a change in the shape of small particles, but it has almost no influence on the shape and on the orientation of the large elongated ones.

6.5. Microstructure of Al_2O_3 -Fe composites

Iron - alumina composites consist of ceramic matrix, particles of iron and FeAl_2O_4 spinel at the particle/matrix interfaces. The Fe particles usually have a spherical shape and are distributed uniformly throughout the matrix as shown in Fig. 32. The results of measurements of particle size and shape in one of such composites are given in Table 5.

It has been also found that size of Fe particles is lower than in the substrate powder. This can be due to the iron melting during the sintering. As a result the

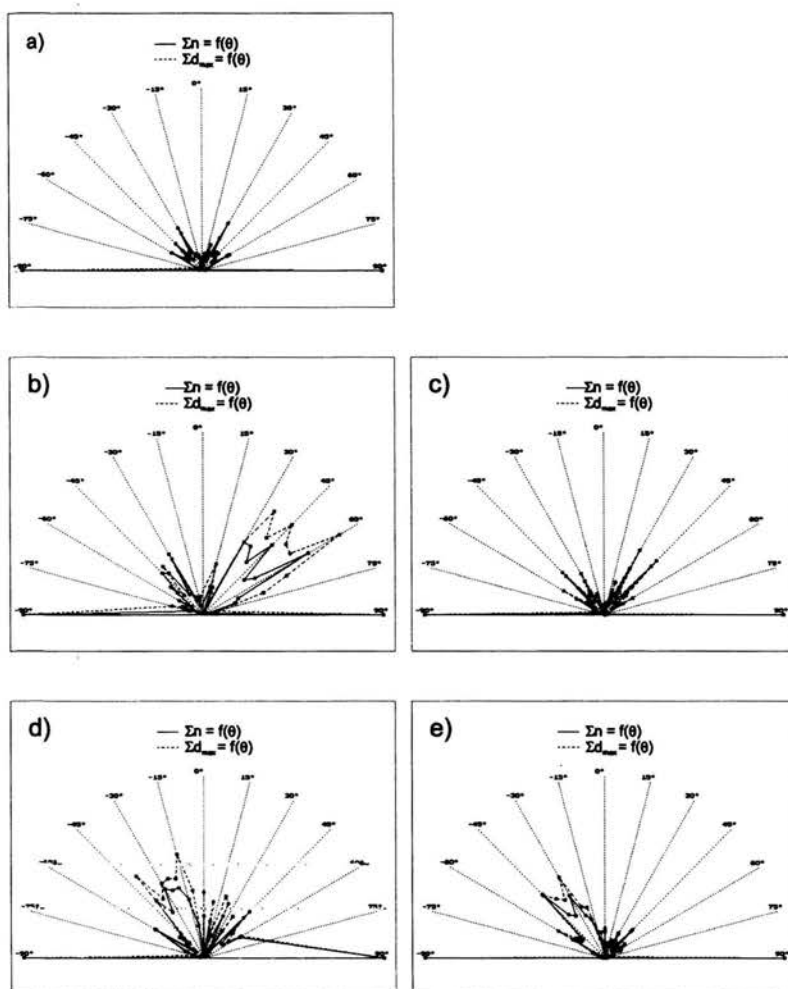


FIGURE 31. Spatial orientation of the Si particle sections quantified in terms of the shape factor weighted number of sections with the orientation of d_{\max} direction within $\omega \pm 3^\circ$ (ω is an angle to the specimen axis) for the specimens of: (a) AS12V, (b) AS12, (c) AS12TT, (d) AS13, (e) AS13TT.

TABLE 5. Results of quantitative analysis of size and shape of Fe particles: d is the mean value of equivalent diameter, d_{\min} and d_{\max} are respectively the mean value of minimum and maximum dimension for planar sections of the composites. The values of the fracture toughness, K_{IC} , are also given.

Sample	d [μm]	d_{\min} [μm]	d_{\max} [μm]	K_{IC} [$\text{MNm}^{-3/2}$]
$\text{Al}_2\text{O}_3 + 10\% \text{Fe}$	23.5 ± 1.2	15.0 ± 0.8	33.1 ± 1.7	5.92 ± 2.12
$\text{Al}_2\text{O}_3 + 30\% \text{Fe}$	25.3 ± 1.3	17.2 ± 0.9	33.2 ± 1.6	5.54 ± 1.19
$\text{Al}_2\text{O}_3 + 50\% \text{Fe}$	22.5 ± 1.1	18.1 ± 0.9	29.1 ± 1.5	4.97 ± 1.42

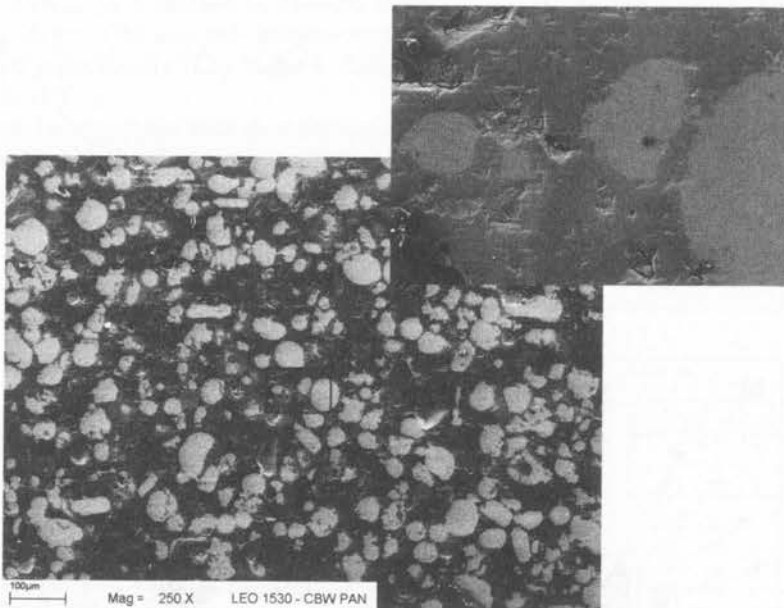


FIGURE 32. SEM images of the microstructure of sintered composite $\text{Al}_2\text{O}_3\text{-Fe}$.

size of Fe particles to some degree can be controlled by the size of the pores available in the sintered material for penetration of the liquid iron.

The fracture toughness of the composites $\text{Al}_2\text{O}_3\text{-Fe}$ is higher than fracture toughness of Al_2O_3 . However, it decreases with increasing content of Fe. A possible explanation of such an effect takes into account the presence of the spinel FeAl_2O_4 . The spinel phase was identified at the metal-ceramic interfaces. It forms during the process of the sintering and weakens the strength of the metal-ceramic interface. As a consequence the composites with more iron are more brittle.

Acknowledgements

The author kindly acknowledges contribution of his colleagues from Department of Materials Science and Engineering of Warsaw University of Technology. Special thanks are to Dr. K. Roźniatowski and Mr. T. Wejrzanowski.

References

1. E.E. UNDERWOOD, *Quantitative Stereology*, Adison Wesley, New York, 1970.
2. K.J. KURZYDŁOWSKI and B. RALPH, *The Quantitative Description of the Microstructure of Materials*, CRC Press Inc., Boca Raton, 1995.
3. J.J. BUCKI and K.J. KURZYDŁOWSKI, Analysis of the effect of grain size uniformity on flow stress of polycrystals, Part I and II, *Materials Characterization*, Vol.29, pp.365-380, 1992.

4. E.B. JENSEN and H.J.G. GUNDERSEN, Stereological ratio estimation based on counts from integral test system, *Journal of Microscopy*, Vol.51, p.125, 1982.
5. E.B. JENSEN and F.B. SORESENSEN, A note on stereological estimation of the volume-weighted second moment of particle volume, *Journal of Microscopy*, Vol.21, p.164, 1991.

